

COLD Fusion: Calibrated and Ordinal Latent Distribution Fusion for Uncertainty-Aware Multimodal Emotion Recognition

Mani Kumar Tellamekala, Shahin Amiriparian, Björn W. Schuller, Elisabeth André, Timo Giesbrecht, Michel Valstar

Abstract—Automatically recognising apparent emotions from face and voice is hard, in part because of various sources of uncertainty, including in the input data and the labels used in a machine learning framework. This paper introduces an uncertainty-aware audiovisual fusion approach that quantifies modality-wise uncertainty towards emotion prediction. To this end, we propose a novel fusion framework in which we first learn latent distributions over audiovisual temporal context vectors separately, and then constrain the variance vectors of unimodal latent distributions so that they represent the amount of information each modality provides w.r.t. emotion recognition. In particular, we impose Calibration and Ordinal Ranking constraints on the variance vectors of audiovisual latent distributions. When well-calibrated, modality-wise uncertainty scores indicate how much their corresponding predictions may differ from the ground truth labels. Well-ranked uncertainty scores allow the ordinal ranking of different frames across the modalities. To jointly impose both these constraints, we propose a softmax distributional matching loss. In both classification and regression settings, we compare our uncertainty-aware fusion model with standard model-agnostic fusion baselines. Our evaluation on two emotion recognition corpora, AVEC 2019 CES and IEMOCAP, shows that audiovisual emotion recognition can considerably benefit from well-calibrated and well-ranked latent uncertainty measures.

Index Terms—Uncertainty Modelling, Dimensional Affect Recognition, Emotion Recognition, Audiovisual Fusion

1 INTRODUCTION

LEARNING to fuse task-specific information from multiple modalities is a fundamental problem in Machine Learning. At its core, this problem entails estimating how informative each modality is towards predicting the labels of a target task. Thus, uncertainty-aware information fusion is a natural approach to multimodal learning. In this work, we formulate an uncertainty-aware fusion method for an inherently multimodal task – apparent emotion recognition from audiovisual signals (faces and voices). We further propose a multimodal fusion framework based on probabilistic modelling of unimodal temporal context.

Being an intrinsically temporal and multimodal phenomenon, continuous emotion (valence and arousal) recognition from face videos and speech signals is one of the long-standing challenges in Affective Computing [1], [2], [3]. A meta-analysis presented in [4] has shown that although emotion recognition can benefit from multimodal fusion

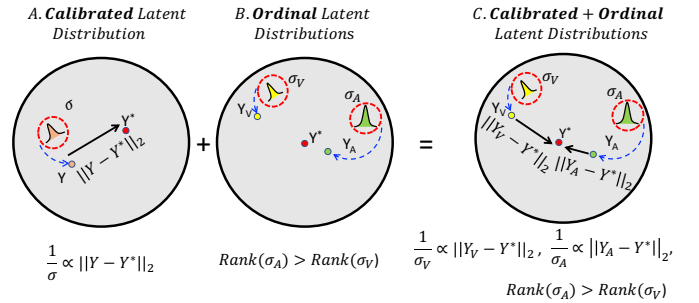


Fig. 1: Illustration of calibration and ordinality constrained latent distributions for multimodal fusion (Y_V and Y_A – unimodal predictions, and Y^* – target label): **A. Calibrated Latent Distributions:** Variance σ represents target informativeness of the latent distribution, so that it is inversely proportional to the expected estimation error $\frac{1}{\sigma} \propto \|Y - Y^*\|_2$, **B. Ordinal Latent Distributions:** Variance values σ_V and σ_A represent their relative target informativeness, to allow ranking of the modalities, and **C. Calibrated + Ordinal Latent Distributions:** Variances of different modalities σ_V and σ_A represent their respective expected estimation errors $\|Y_V - Y^*\|_2$ and $\|Y_A - Y^*\|_2$, and simultaneously allow ordinal ranking of the unimodal latent distributions.

in general, performance improvements are not significant when it comes to spontaneous emotions. We believe that uncertainty-aware multimodal fusion may have the potential to address this challenge, considering that the intensity of spontaneous emotions embedded in the facial and vocal

- Mani Kumar Tellamekala and Michel Valstar are with the Computer Vision Lab, School of Computer Science, University of Nottingham, UK. E-mail: {mani.tellamekala, michel.valstar}@nottingham.ac.uk
- Shahin Amiriparian and Björn W. Schuller are with the Chair of Embedded Intelligence for Health Care & Wellbeing, University of Augsburg, Germany. Björn W. Schuller is also with the GLAM – the Group on Language, Audio, & Music, Imperial College London, UK. Email: {shahin.amiriparian, schuller}@uni-a.de
- Elisabeth André is with the Chair for Human-Centered Artificial Intelligence, University of Augsburg, Germany. E-mail: andre@informatik.uni-augsburg.de
- Timo Giesbrecht is with Unilever R&D Port Sunlight, UK. Email: timo.giesbrecht@unilever.com

Manuscript submitted on June 12, 2022

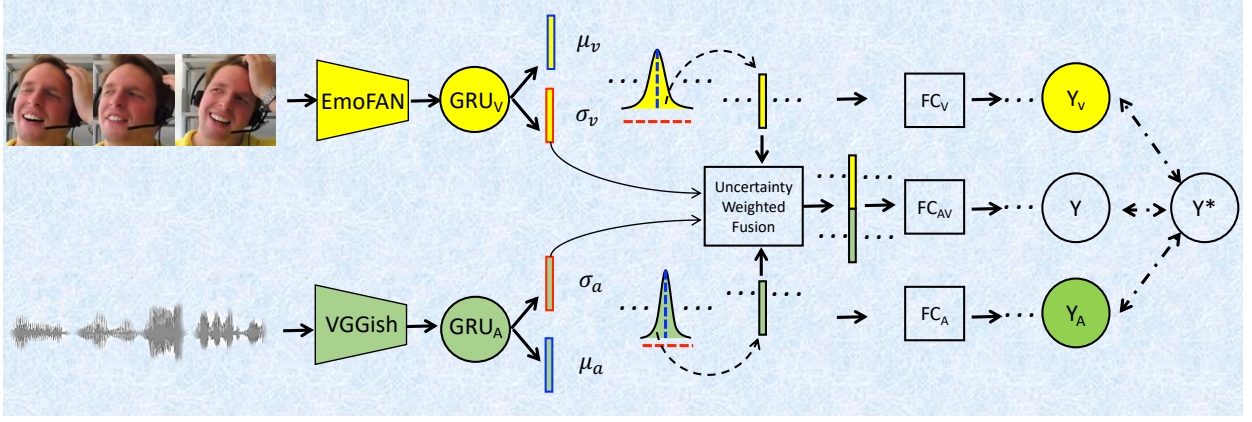


Fig. 2: Overview of the proposed approach to an uncertainty-aware audiovisual fusion for emotion recognition: Modelling latent distributions over unimodal temporal context vectors to derive modality-wise uncertainty guided fusion weights. A detailed description of our approach is given in Section 3.

expressions are likely to vary dynamically over time [5], [6].

Although Deep Neural Networks (DNNs) have been extensively applied to audiovisual emotion recognition [7], [8], [9], [10], estimating modality-wise uncertainty for improved fusion performance is a relatively unexplored avenue. However, modelling predictive uncertainty (or confidence, its opposite) in DNNs received widespread attention in recent years [11], [12], motivated by the observation that DNNs tend to make over-confident predictions [13], [14]. Most existing efforts towards uncertainty or confidence estimation in DNNs [11], [15] focus solely on reducing miscalibration errors, i.e., the mismatch between expected model estimation errors and according confidence scores. Recently, as an alternative perspective, Moon et al. [16] introduced the idea of learning to rank confidence scores for identifying the most reliable predictions.

Our objective is to estimate the uncertainty scores of unimodal inputs to maximise the multimodal fusion performance. We argue that the predictive uncertainty of an estimator must be simultaneously both *well-calibrated* and *well-ranked (ordinal)*. The former is needed to accurately represent the correctness likelihood of a prediction for **an individual sample**. The latter is essential to effectively order predictions for **a group of samples** according to their correctness likelihoods. In other words, if an uncertainty estimate of an individual sample is well-calibrated, in the absence of its ground truth, the uncertainty score can serve as a proxy for its expected prediction error. If the uncertainty scores associated with different predictions are well-ranked or maintain ordinality, then one can use them to order their corresponding samples in terms of their reliability towards the target prediction, and to distinguish the most informative samples from the least informative samples.

For multimodal temporal learning, it is critical to estimate how informative the predictions made for different frames in different unimodal sequences are, towards estimating a common target label, so that the target-specific information can be reliably integrated [17]. In this work, we hypothesise that jointly learning these two properties – calibration and ordinality – may lead to more reliable per-frame predictive uncertainty estimates for each modality,

facilitating more effective uncertainty-weighted temporal context fusion. Based on this hypothesis, we propose an uncertainty modelling method that imposes the calibration and ordinality constraints jointly, as Figure 1 illustrates. We condition the unimodal latent distributions’ variance vectors such that they represent the informativeness of different modalities w.r.t. predicting the target labels. Our proposed method can be viewed as an uncertainty-aware extension of classical late fusion. We propose to learn uncertainty estimates in terms of higher dimensional, more informative, latent distributions, unlike simple confidence-weighted late fusion which directly models uncertainty over lower-dimensional (less informative) unimodal predictions. We presume that modelling uncertainty in the higher dimensional latent space may be more effective than in the lower dimensional label space.

In our proposed framework, denoted as Calibrated Ordinal Latent Distributions (COLD), we first learn the latent distributions (multivariate normal distributions) over the temporal context of audio and visual modalities separately, as Figure 2 shows. We model the variance values of the audio and visual latent distributions, σ_V and σ_A , as the confidence measures towards emotion prediction. We design a novel training objective based on softmax distributional matching to encourage the frame-wise variance values in each modality to be: (a) inversely correlated with the correctness likelihood of the unimodal predictions, and (b) ordinal in nature to effectively rank the frames of both the modalities towards the target prediction. Thus, the calibrated and ordinal unimodal variance scores are learnt for effective uncertainty-weighted fusion, as shown in Figure 2.

We evaluate the proposed COLD fusion on two large-scale audiovisual corpora, AVEC 2019 CES [3] and IEMO-CAP [18], for recognising spontaneous and acted emotions respectively. The experimental results show that the COLD fusion outperforms the standard model-agnostic fusion baselines by large margins, with $\sim 6\%$ average relative improvement over the best performing fusion baseline trained for emotion regression. Furthermore, we assess the robustness of different fusion models at test time by inducing noise into the visual modality through face masking. With the

faces masked in 50% of the evaluation sequences, the COLD fusion achieves $\sim 17\%$ average relative improvement over the best fusion baseline.

The key contributions of our work are as follows:

- We propose an uncertainty-aware multimodal fusion method that dynamically estimates informativeness of unimodal inputs w.r.t. target label prediction.
- We demonstrate how to jointly learn *well-calibrated* and *well-ranked* unimodal uncertainty measures. For this purpose, we propose a simple softmax distributional matching loss function that applies to both regression and classification models.
- On two standard audiovisual emotion recognition databases, our fusion model outperforms the standard model-agnostic fusion baselines as well as a multimodal transformer baseline.

2 RELATED WORK

Audiovisual Dimensional Affect Recognition. Humans rely primarily on visual (faces) and audio (voices) modalities to encode and express their affective or emotional states. Recognising dimensional emotions, valence (how pleasant an emotion is) and arousal (how active an emotion is), from audiovisual modalities is a widely studied problem in various prior works [6], [19], ranging from the almost a decade-long running annual AVEC challenge series [1], [2], [3] to the recently introduced MuSe challenge [20], [21], [22] and ABAW challenge [23], [24]. We refer the reader to Poria et al. [25] and Roust et al. [7] for comprehensive surveys of affect recognition in multimodal settings and contemporary deep learning-specific advancements in it. Since our main focus in this work is on uncertainty-aware fusion models for emotion recognition, we review the literature closely related to the following key research topics: i) uncertainty modelling for emotion and expression recognition, ii) uncertainty-aware multimodal fusion, iii) calibrated uncertainty, and iv) ranking-based uncertainty.

Uncertainty Modelling for Emotion and Expression Recognition. In discrete facial expression recognition tasks, modelling predictive uncertainty is studied in several recent works [26], [27], [28], by estimating uncertainty in the space of low-dimensional feature embedding outputs from a Convolutional Neural Network (CNN) backbone. On the other hand, directly predicting emotion label uncertainty is explored in [29], but only in unimodal (video-only) settings. For uncertainty-aware multimodal emotion recognition, some prior works applied Kernel Entropy Component Analysis (KECA) [30] and Multi Modal-Hidden Markov Models (MM-HMMs) [31] by predicting modality-specific uncertainty measures for estimating the fusion weights.

Noting the limitations of deterministic function learning in DNNs for uncertainty modelling, Dang et al. [32] explored the application of Gaussian Process (GP) Regression to the fusion of emotion predictions. With the same motivation, in Affective Processes (APs) [33], [34], Neural Processes [35], [36] have been applied to the task of emotion recognition. By combining the abilities of GPs to learn function distributions with DNN's representation learning abilities, APs demonstrated superior generalisation performance over deterministic function learning models.

Building on this idea of stochastic modelling of temporal functions, recently Affective Processes have been extended to multimodal settings in [37] based on a strictly model-based fusion approach, demonstrating impressive emotion recognition results. However, for uncertainty-aware temporal context modelling, APs heavily rely on the proxy labels predicted by a separate pre-trained backbone, and a complex encoder-decoder formulation. In contrast to APs, our method aims to model the temporal context uncertainty in the model-agnostic fashion, by just altering the output head of simple CNN+RNN models that are trained using some novel constrained optimisation objectives.

All the aforementioned methods demonstrated the potential of uncertainty-aware emotion recognition models over their uncertainty-unaware counterparts in general. However, they ignore two important aspects in uncertainty modelling: calibration and ordinality (ranking). In this work, we aim to demonstrate the significance of these two properties by hypothesising that learning well-calibrated and well-ranked uncertainty estimates is critical for improving the audiovisual emotion recognition performance.

Uncertainty-Aware Multimodal Fusion. In general, for multimodal sensor fusion, several prior works [30], [38], [39], [40] explored uncertainty-aware or confidence-weighted averaging techniques for classic machine learning models before the advent of Deep Neural Networks (DNNs). Recently, Subedar et al. [41] applied Bayesian DNNs for uncertainty-aware audiovisual fusion to improve human activity recognition performance. Similarly, Tian et al. [42] explored the use of uncertainty estimation in fusing the softmax scores predicted using CNNs for semantic segmentation. Although these approaches demonstrated critical advantages over the models that predict only point estimates, they do not study the calibration properties of the estimated uncertainty scores. Further, such DNN models focus mainly on modelling absolute uncertainty estimates, whereas our focus is on jointly **learning the calibrated and relational uncertainty estimates** in an end-to-end fashion introducing a novel loss function based on softmax distributional matching.

Calibrated Uncertainty. As DNNs tend to make overconfident predictions [13], [14], confidence calibration has received significant attention in recent years [13], [14]. Calibrating confidence or uncertainty estimates involves maximising the correlation between predictive accuracy values and predictive uncertainty scores. A wide variety of calibration techniques, particularly in classification settings, can be broadly categorised into explicit and implicit calibration categories [43]. In the former category, two types of post-hoc methods, binning-based and temperature-scaling, are applied to increase the reliability of DNN confidence estimates [11], [44]. In binning-based methods such as non-parametric histogram binning [45], calibrated confidence is estimated based on the average count of positive-class instances in each bin. This method is extended to jointly optimise the bin boundaries and their predictions in Isotonic Regression [46]. Temperature-scaling methods can be viewed as generalised versions of Platt scaling [47] using logistic regression for calibrating the class probabilities. We use temperature-scaling as a calibration baseline [11], [48] to compare against the uncertainty calibration performance of

the proposed method, due to its simplicity.

Implicit calibration methods mainly focus on tailoring the training objective of DNNs to minimise the prediction error and calibration error simultaneously. Addressing the limitations of standard cross-entropy loss w.r.t. confidence calibration, various alternative loss functions such as focal loss [12], maximum mean calibration error [15], and accuracy vs uncertainty calibration [49], have been investigated recently. Calibrating regression models is relatively under-explored compared to the classification. Some recent works [50], [51], [52] made attempts to extend some of the aforementioned calibration techniques to continuous-valued predictions.

Ordinal or Ranking-based Uncertainty. In the existing uncertainty modelling works, the ordinal property of uncertainty estimates received less attention compared to the calibration property, which partly motivated the method introduced in this paper. Li et al. [53] proposed to model data uncertainty by inducing ordinality into probabilistic embeddings of face images. Towards uncertainty-aware regression problems, the results reported in [53] highlighted the key limitations of deterministic unordered embeddings compared to the probabilistic ordinal embeddings. Although not strictly ordinal, relative uncertainty modelling is explored for facial expression recognition in [27].

Other closely related works approached the problem of ordinal ranking of uncertainty estimates with different objectives such as failure prediction [54], out-of-distribution detection [55], and selective classification [56]. Fundamentally, all these objectives necessitate a method that can train the model to output well-ranked confidence or uncertainty scores. Among these existing methods, the one most closely related to ours is by Moon et al. [16], which proposes a Correctness Ranking Loss (CRL). CRL directly imposes ordinal ranking constraints on the confidence estimates of a DNN classifier. Similar to CRL, our proposed softmax distributional matching loss also constrains the ordinal-ranking property of uncertainty estimates. However, in addition to ordinal ranking, our method imposes the calibration property as well, most importantly by controlling the latent distribution variance, unlike in CRL. Moreover, our formulation generalises the idea of calibrated and ordinal uncertainty estimates to both classification and regression settings, using a common loss function computation.

3 MODEL-AGNOSTIC FUSION BASELINES

Before introducing our uncertainty-aware multimodal fusion formulation, we briefly discuss the general multimodal fusion techniques w.r.t. audiovisual emotion recognition and introduce the related notations. One fundamental question in multimodal learning concerns the optimal stage to perform fusion [57]. In this work, we consider the following three typical model-agnostic fusion methods as the standard baselines: feature fusion, temporal context fusion, and prediction fusion.

Preliminaries and Notations. As Fig. 2 illustrates, given a face video clip X_V with N frames and its corresponding speech signal X_A , using overlapping time windows, we first create N speech segments that correspond to the N visual frames. Here, we assume that both the signals X_V and X_A

are annotated with a common dimensional emotion label, $Y^* = [Y_{valence}^*, Y_{arousal}^*]$ (either per-frame or per-sequence). We extract sequences of per-frame low dimensional features (Z_V, Z_A) from the face video and speech inputs using a two-stream network. This network is composed of a 2D CNN f_V and a 1D CNN f_A for processing the face images and speech segments respectively, $f_V : X_V \rightarrow [z_V^1, z_V^2, \dots, z_V^N]$ and $f_A : X_A \rightarrow [z_A^1, z_A^2, \dots, z_A^N]$. For unimodal emotion recognition, we process the temporal context from each modality separately from Z_V and Z_A using different temporal networks $g_V : Z_V \rightarrow Y_V$ and $g_A : Z_A \rightarrow Y_A$ to predict the emotion labels Y_V and Y_A .

Feature Fusion or early fusion integrates frame-level emotion cues present in the audiovisual features Z_V and Z_A (e.g., [58]), not accounting for commonly encountered temporal misalignment between different modalities [59]. Here, we concatenate the per-frame audiovisual features into a single sequence, $Z = [Z_V, Z_A]$, then pass it to a common temporal network $g_{AV} : Z \rightarrow Y$ to predict emotion labels.

Decision Fusion combines the unimodal emotion predictions Y_V and Y_A (e.g., [60]). Here, we apply predictive confidence based weighted averaging to perform the late fusion. Unlike early fusion, late fusion does not leverage the low-level correspondences among the emotion cues distributed over the audio and visual streams [57].

Temporal Context Fusion or simply context fusion integrates sequence-level emotion information aggregated in the form of audiovisual temporal context vectors h_V^i and h_A^i for frame i , produced by the temporal networks g_V and g_A respectively. This method is also referred to as ‘feature fusion with RNNs’ or ‘mid-level’ fusion in some prior works [7], [61]. It is important to note that here, temporal context or simply context at i^{th} frame refers to the emotion information present in frame i w.r.t. the emotion information carried by remaining frames in the input sequence. As a result, unlike early fusion, context fusion is bound to suffer less from the temporal misalignment between the emotion-related semantics of audio and visual feature sequences. Further, context fusion benefits from the low-level audiovisual correspondences in the emotion space, in contrast to late fusion.

Considering the above mentioned critical advantages of temporal context fusion, in this work, we propose to learn an uncertainty-aware context fusion model for multimodal emotion recognition as discussed below.

4 PROPOSED METHOD

Figure 3 illustrates our proposed solution to uncertainty-aware multimodal fusion. In this section, we first discuss how we estimate modality-wise uncertainty by learning unimodal latent distributions over the temporal context, and we present our approach to derive the audiovisual fusion weights based on unimodal context variance. Then, we introduce two key optimisation constraints that are imposed on the variance norms of unimodal latent distributions and discuss their implementation details.

4.1 Uncertainty-Aware Audiovisual Context Fusion

Quantifying modality-wise uncertainty towards predicting a common target label is crucial to improve the multimodal

fusion performance. Our objective is to first quantify intramodal uncertainty in the temporal context space, and then use the estimated uncertainty scores to derive the fusion weights. To this end, we propose to learn unimodal latent distributions over the temporal context of the audio and visual modalities separately, as discussed below.

4.1.1 Latent Distributions over Unimodal Temporal Context

Figure 2 illustrates how we modify the temporal networks (Gated Recurrent Unit(GRU)-RNNs) g_V and g_A to output the parameters (mean and variance) of multivariate normal distributions $\mathcal{N}(\mu_V^i, \sigma_V^i)$ and $\mathcal{N}(\mu_A^i, \sigma_A^i)$ over the audio and visual temporal context vectors, respectively. Here, the term ‘temporal context’ refers to the hidden state outputs from the corresponding unimodal GRU blocks (g_A or g_V). For each modality separately, we learn this hidden state output as a multivariate normal distribution, instead of a typical deterministic embedding vector. We presume that these unimodal latent distributions are capable of representing modality-wise emotion information more effectively than deterministic embeddings.

We model the variance of a unimodal latent distribution as a proxy for how informative that modality is w.r.t. predicting the target emotion, and we use the inverse of variance values to quantify how uncertain a particular modality is towards predicting emotion labels. Note that the potential of signal variance-based uncertainty modelling for multimodal fusion was already demonstrated in [62]. Similarly, learning latent distribution variance was determined to be capable of uncertainty modelling in [33]. Inspired by these ideas, we model the unimodal context variance values σ_A and σ_V to estimate how certain the audio and visual modalities are about predicting the emotion labels. Our approach to derive variance-based fusion weights for integrating the audiovisual temporal context vectors is discussed below.

4.1.2 Context Distribution Variance-Based Fusion Weights

For an input frame with index i , given its unimodal latent distributions $\mathcal{N}(\mu_V^i, \sigma_V^i)$ and $\mathcal{N}(\mu_A^i, \sigma_A^i)$ over its audio and visual temporal context separately, we first compute the $L2$ norms of their variance values $\|\sigma_V^i\|_2$ and $\|\sigma_A^i\|_2$. As discussed above, these variance norm values are assumed to represent modality-specific certainty or informativeness w.r.t. predicting the target emotions. By normalising the variance norm values of the audio and visual modalities, we derive fusion weights that are used in a simple linear fusion model of the audiovisual temporal context (h_{VA}^i):

$$h_{VA}^i = w_V^i * h_V^i + w_A^i * h_A^i, \quad (1)$$

where h_V^i and h_A^i denote the visual and audio temporal context vectors, and w_V^i and w_A^i denote their corresponding weight values. The temporal context vectors h_V^i and h_A^i are sampled from their respective latent distributions, $h_V^i \sim \mathcal{N}(\mu_V^i, \sigma_V^i)$ and $h_A^i \sim \mathcal{N}(\mu_A^i, \sigma_A^i)$ during training. At test time, we set h_V^i and h_A^i to their corresponding mean vectors μ_V^i and μ_A^i for evaluation purpose.

Based on the unimodal context variance norm values ($\|\sigma_V^i\|_2$ and $\|\sigma_A^i\|_2$), the weight values w_V^i and w_A^i in Equation (1) are computed as:

$$w_V^i = \frac{\|\sigma_V^i\|_2}{(\|\sigma_V^i\|_2 + \|\sigma_A^i\|_2)}, w_A^i = \frac{\|\sigma_A^i\|_2}{(\|\sigma_V^i\|_2 + \|\sigma_A^i\|_2)}. \quad (2)$$

Context variance modelling seems to be a simple yet effective approach to uncertainty-aware audiovisual fusion, yet learning audiovisual latent distributions with well-conditioned variance ranges is non-trivial in practice, as we show later in the experiments. To condition the variance values that can effectively capture intramodal uncertainty w.r.t. predicting the target labels, we define a more principled model training that applies two key optimisation constraints: Calibration and Ordinality.

4.2 COLD: Calibrated and Ordinal Latent Distributions

To effectively learn the unimodal latent distributions for uncertainty-aware fusion, we propose to condition their variance values by applying optimisation constraints to the model training objective. We achieve this conditioning by imposing two key constraints: Calibration and Ordinality (or ranking) on the latent distribution variance vectors. When well-calibrated, an uncertainty score acts as a proxy for the correctness likelihood of its prediction for an individual input from a specific modality. In other words, well-calibrated uncertainty indicates the expected estimation error, i.e., how far the predicted emotion is expected to lie from its ground truth.

Given the predictions made for a set of frames from different modalities, when their uncertainty scores are well-ranked or maintain ordinality, we can effectively arrange the input unimodal frames according to their reliability for predicting a target emotion. In Figure 1, we illustrate the definitions of both these constraints. *It is important to note the fundamental difference between these two constraints: while the calibration constraint is applied individually for each unimodal frame, the ordinality or ranking constraint is imposed jointly for a set of frames from different modalities.*

Calibration Constraint – this is imposed by regularising the unimodal context variance norm values, $\|\sigma_V^i\|_2$ and $\|\sigma_A^i\|_2$, such that they are proportional to the correctness likelihood values of target emotion classes. In regression models, this constraint can be implemented by forcing the variance norm values to be directly proportional to the Euclidean distance between their corresponding unimodal predictions Y_V and Y_A and their ground truth labels Y , as shown in Fig. 1. In other words, the context variance values are learnt as reliability measures indicating how far the emotion predictions are expected to lie from their ground truth labels. To impose this property on the variance values of both modalities, we apply the following regularisation constraints,

$$\frac{1}{\|\sigma_V^i\|_2} \propto d(Y_V, Y^*), \frac{1}{\|\sigma_A^i\|_2} \propto d(Y_A, Y^*), \quad (3)$$

where $d(\cdot)$ denotes the distance function that measures the target emotion estimation error. We use cross-entropy and Mean Squared Error (MSE) as the distance functions for the classification and regression models respectively.

Ordinality Constraint – this is applied to rank the frames of unimodal sequences, so that their uncertainty measures indicate how reliable different unimodal frames are w.r.t.

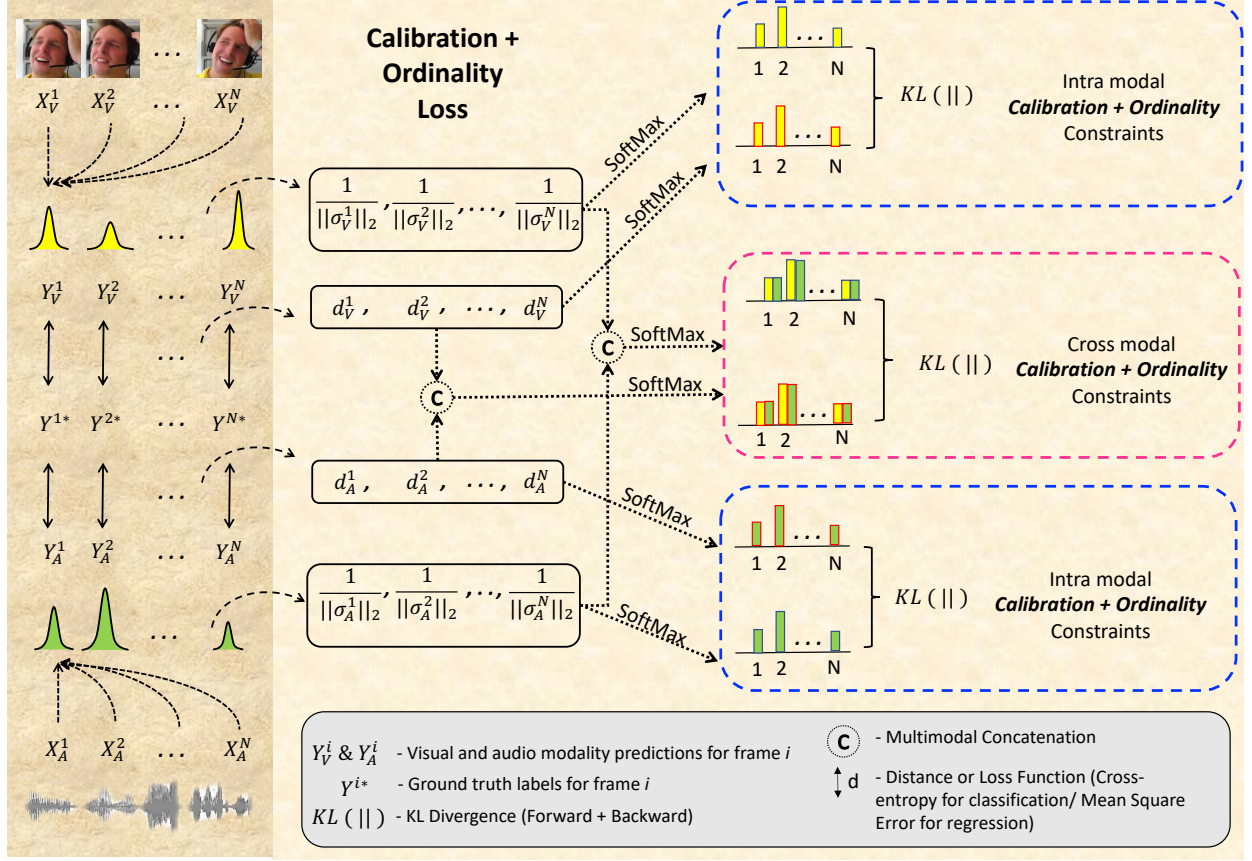


Fig. 3: COLD fusion training loss computation: To simultaneously impose the calibration and ordinality constraints on the unimodal latent distributions' variance vectors, we minimise the softmax distributional matching loss (KL divergence) between the distance vectors $[d^i]$ and variance-norm vectors $[\frac{1}{\|\sigma^i\|_2}]$, in both intramodal and crossmodal settings.

each other. This ranking operation can be implemented as a simple ordering constraint which jointly regularises the unimodal context variance norm values, $\|\sigma_V^i\|_2$ and $\|\sigma_A^i\|_2$. Here, modality-wise reliability is again computed using the inverse of distance function (see Equation (3)) between different unimodal predictions and the ground truth labels:

$$\text{Rank}\left(\frac{1}{\|\sigma_V^i\|_2}, \frac{1}{\|\sigma_A^i\|_2}\right) \propto \text{Rank}(d(Y_V, Y^*), d(Y_A, Y^*)). \quad (4)$$

4.2.1 Implementation: Calibration and Ordinality Constrained Training for Audiovisual Emotion Recognition

We train classification models of dimensional emotion recognition, in addition to the standard regression models used in the literature. In both cases, the underpinning principles of the COLD fusion are the same, but implementations of the training objective differ slightly. To train the temporal context fusion models by imposing the above-described calibration and ordinality constraints, we optimise the network to jointly minimise a loss function composed of the following components:

Emotion Prediction Loss (L_{emo}) is computed using the standard cross-entropy function for training the classification models. For the regression models training, similar to [63], we use inverse Concordance Correlation Coefficient (CCC) loss ($1.0 - \text{CCC}$) in addition to MSE. This loss is

computed for the predictions from unimodal (Y_V and Y_A) and multimodal (Y_{AV}) branches jointly (Figure 2).

Calibration and Ordinality Loss (L_{CO}) combines the aforementioned constraints, defined in Equation (3) and Equation (4), into a single training objective using differentiable operations. Figure 3 shows the steps involved in implementing this component: given an input sequence with N frames, we first compute their unimodal latent distributions followed by their corresponding unimodal predictions. To impose the calibration and ordinality constraints, we first compute two sets of vectors for each modality:

Distance Vectors. We collect the scalar distance values (d_V^i and d_A^i) between the unimodal predictions (Y_V^i and Y_A^i) and the ground truth labels (Y^{i*}) using either cross-entropy (classification) or MSE (regression) as the distance function. This step produces N -dimensional distance vectors, $D_V = [d_V^1, d_V^2, \dots, d_V^N]$ and $D_A = [d_A^1, d_A^2, \dots, d_A^N]$.

Variance-Norm Vectors. We collect the inverted unimodal context variance norm values into another set of N -dimensional vectors, S_V and S_A , as shown below:

$$S_V = \left[\frac{1}{\|\sigma_V^1\|_2}, \frac{1}{\|\sigma_V^2\|_2}, \dots, \frac{1}{\|\sigma_V^N\|_2} \right] \quad (5)$$

$$S_A = \left[\frac{1}{\|\sigma_A^1\|_2}, \frac{1}{\|\sigma_A^2\|_2}, \dots, \frac{1}{\|\sigma_A^N\|_2} \right].$$

Softmax Distributional Matching for Calibration and Ordinal Ranking. Note that the distance vectors and

variance-norm vectors contain scalar values that summarise the properties of different embedding spaces, emotion labels, and temporal context, respectively. Hence, we assume that matching their properties by imposing the calibration and ordinality constraints directly in their original spaces, is not optimal. For this reason, as illustrated in Figure 3, we first apply the softmax operation on the distance vectors and variance-norm vectors separately to generate the softmax distributions. Then, we impose the calibration and ordinality constraints by minimising the mismatch between softmax distributions of the variance-norm vectors and distance vectors. This approach to calibration and ordinality loss computation based on soft-ranking is inspired by [64] in which softmax cross-entropy is used for ordinal regression.

As Figure 3 shows, in both intramodal and crossmodal settings, we compute the softmax distributions of distance vectors (P_{D_V} , P_{D_A} , and $P_{D_{AV}}$) and variance-norm vectors (P_{S_V} , P_{S_A} , and $P_{S_{AV}}$). Note that in the crossmodal case, we first concatenate the audio and visual distance vectors and variance-norm vectors separately, i.e., $D_{AV} = [d_A^1, d_V^1, \dots, d_A^N, d_V^N]$ and $S_{AV} = [s_A^1, s_V^1, \dots, s_A^K, s_V^K]$. Then, we apply the softmax operation on the concatenated list which is $2N$ dimensional. Thus, the crossmodal softmax distributions capture the relative measures across both modalities. Now, to impose the calibration constraint, we minimise the KL divergence (both forward and backward) between the distance distributions and variance-norm distributions in both intramodal and crossmodal settings, as shown below:

$$L_{CO} = KL(P_D || P_S) + KL(P_S || P_D), \quad (6)$$

where P_D represents P_{D_V} and P_{D_A} , and P_S represents P_{S_V} and P_{S_A} in the intramodal loss computation. In the crossmodal case, P_D and P_S denote $P_{D_{AV}}$ and $P_{S_{AV}}$, respectively.

Variance Regularisation Loss (L_{regu}). Prior works [33], [65] on latent distribution learning in high-dimensional input spaces such as images, have reported that the variance collapse is a commonly encountered problem. Variance collapse occurs mainly because the network is encouraged to predict small variance σ values to suppress the unstable gradients that arise while training the latent distribution models using Stochastic Gradient Descent. To prevent this problem, we include the regularisation term proposed in [65] in the training objective:

$$\begin{aligned} L_{regu} &= KL(\mathcal{N}(\mu, \sigma) || \mathcal{N}(\epsilon, \mathbf{I})) \\ &= -\frac{1}{2}(1 + \log \sigma^2 - \mu^2 - \sigma^2), \end{aligned} \quad (7)$$

where ϵ and \mathbf{I} denote the mean vector and an identity variance matrix respectively. Note that this regularisation term is applied to the audio and visual context latent distributions, separately.

In summary, the COLD fusion training objective composed of the above-discussed loss components, is as follows:

$$L_{total} = L_{emo} + \lambda_{CO_V} \cdot L_{CO_V} + \lambda_{CO_A} \cdot L_{CO_A} + \lambda_{CO_{AV}} \cdot L_{CO_{AV}} + \lambda_R \cdot L_{regu}, \quad (8)$$

where λ_{CO_V} , λ_{CO_A} , $\lambda_{CO_{AV}}$, and λ_R are the optimisation hyperparameters that control the strength of each regularisation constraint.

5 EXPERIMENTS

We first discuss the details of dimensional emotion recognition datasets used for evaluating the proposed COLD fusion model. Detailed information about each dataset can be found in [3], [18]. Then, we discuss the regression and classification formulations of emotion recognition and their corresponding performance evaluation metrics, along with a standard uncertainty calibration error metric that applies to the classification models. Finally, we present the details of the network architectures, fusion model implementations, and their optimisation.

5.1 Datasets

For Spontaneous Emotion Recognition, we used the AVEC 2019 CES challenge corpus [3] which is designed for in-the-wild emotion recognition in cross-cultural settings as part of the SEWA project [66]. This corpus is composed of 8.5 hours of audiovisual recordings collected from German, Hungarian, and Chinese participants. All videos in this corpus are annotated with continuous-valued valence and arousal labels in the range $[-1, 1]$. Note that the train and validation partitions are composed of only German and Hungarian cultures. As the labels for the test set (which has the Chinese culture in addition) are not publicly available, we report results on the validation set.

For Acted Emotion Recognition, the Interactive Emotional Dyadic Motion Capture (IEMOCAP) dataset [18] is used. This dataset constitutes 12 hours of audiovisual data annotated with utterance-level labels of valence and arousal. Here, we normalised the original emotion labels to the range $[-1, 1]$. Among the available five sessions in this corpus, we used the first four sessions' data for training. Note that the COLD fusion model training involves tuning of multiple regularisation constraints (Equation (8)). Thus, the usual 5-fold cross-validation evaluation is found to be computationally expensive as it requires the values of λ_{CO_V} , λ_{CO_A} , $\lambda_{CO_{AV}}$, and λ_R to be tuned for every fold. For this reason, we used the speaker-independent partitions of the fifth session as validation and test sets, same as the first fold's validation and test sets used in the existing works (e.g. [67], [68]) that apply 5-fold cross validation.

On both the emotion datasets we trained and evaluated our audiovisual fusion models in regression as well as classification settings. To train the regression models, we directly used the continuous-valued labels as targets in the range $[-1, 1]$. For classification, we first mapped the continuous emotion values to three different classes for valence (positive, neutral, negative) and arousal (high, neutral, low) individually. For this binning, we chose the thresholds of -0.05 and 0.05 to draw the boundaries between the three above-mentioned bins. We adjusted the binning thresholds and picked the aforementioned values, to minimise the imbalances in the resultant class-wise label distributions.

Addressing Imbalanced Emotion Class Label Distributions. Despite carefully tuning the binning thresholds, class-wise label distributions for both datasets still have significant imbalances, as shown in Figure 4. To mitigate the effect of this problem, we applied two general techniques while training the classification models: a. non-uniform sampling

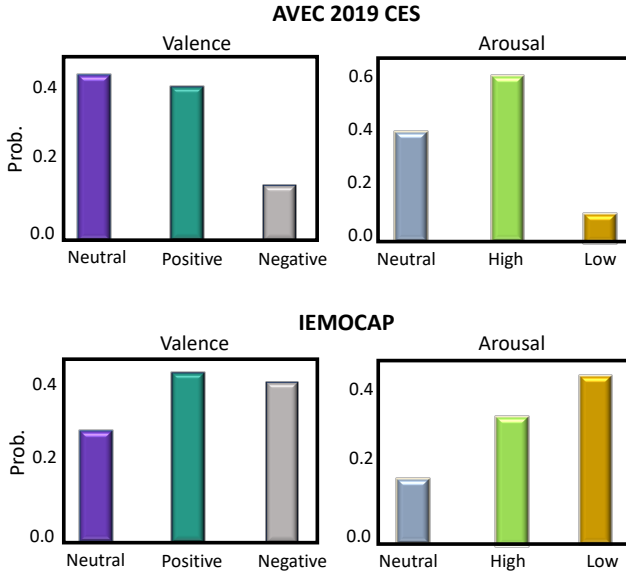


Fig. 4: Class imbalances in the distributions of valence and arousal labels prepared for 3-way classification on the AVEC 2019 CES and IEMOCAP datasets.

of the training instances for different classes and b. class-weighted cross-entropy loss. In the former, we modified the sampling criteria to oversample for the minority classes and undersample for the majority classes based on the number of examples available for each class in the train set. In the latter technique, we divided the cross-entropy loss values for different classes by their relative bin size (in the train set).

5.2 Evaluation Metrics

Regression models' performance is measured using Lin's Concordance Correlation Coefficient (CCC) [69] between the predicted emotions y^o and their ground truth labels y^*

$$CCC = \frac{\rho_{y^*y^o} \cdot \sigma_{y^*} \cdot \sigma_{y^o}}{(\mu_{y^*} - \mu_{y^o})^2 + \sigma_{y^*}^2 + \sigma_{y^o}^2}, \quad (9)$$

where $\rho_{y^*y^o}$ denotes the Pearson's coefficient of correlation between y^* and y^o , and (μ_{y^*}, μ_{y^o}) and $(\sigma_{y^*}, \sigma_{y^o})$ denote their mean and standard deviation values, respectively.

Classification models are evaluated using precision, recall, and F1 score metrics, given that accuracy is not a reliable metric because of the imbalanced class distributions (see Figure 4). In all three metrics, we compute the unweighted values or macro average values of the three emotion classes, for the valence and arousal dimensions separately.

Uncertainty Calibration Errors of the classification models are measured to analyse the deviations between the true class likelihoods p and the predicted class confidence estimates \hat{p} . Reliability diagrams [11] are used as empirical approximations to visually represent the confidence calibration errors. For plotting these diagrams, first, the accuracy and confidence axes are binned into equally-sized intervals and then, for each interval mean accuracy values are plotted against their corresponding mean confidence scores. For a

perfectly calibrated model, the reliability diagram is supposed to be an identity function, i.e., accuracy and confidence should have the same values. Expected Calibration Error (ECE), a scalar summary statistic of the reliability diagram, computes the weighted average of calibration errors over all the intervals in a reliability diagram.

$$ECE = \sum_{m=1}^M \frac{|I_m|}{N} |Acc(I_m) - Conf(I_m)|, \quad (10)$$

where I_m denotes the m^{th} interval, M is the total number of intervals, and N is the total number of samples.

5.3 Network Architectures

Visual CNN Backbone. EmoFAN [70], a 2D CNN proposed recently for facial feature extraction, is proved highly efficient by building on hour-glass-based network architectures. This CNN backbone, pretrained on 2D face alignment task, has been found very efficient for transfer learning tasks [71], [72]. We used its pretrained model¹ on image-based emotion recognition on the AffectNet dataset [73]. Using this backbone, we extracted a 512D feature vector per frame.

Audio CNN Backbone. We adopted a 2D CNN backbone proposed in [74] for extracting speech signal features in an end-to-end fashion. Here, we applied a VGGish [75] pretrained module to 2D Mel-spectrograms that are derived by setting the hop size and window length values to 0.1 s and 1 s respectively. Similar to [74], we fine-tuned only the last two fully connected layers of this VGGish module. To differentiate the interlocutor's information from that of the target speaker, we implemented the feature dimensionality-doubling technique proposed in [76].

Temporal Networks are stacked on top of the unimodal CNN backbones to model the temporal dynamics and integrate the multimodal affect information. Note that all the fusion models evaluated in this work follow different temporal network implementations. However, all the temporal networks have the following GRU block in common: a 2-layer bidirectional GRU module followed by a fully connected (FC) output layer. This GRU block contains 256 hidden units with the dropout value set to 0.5. The number of GRU blocks and their input-output dimensionality vary across different fusion models, as discussed below.

In feature fusion, a single GRU+FC block is used to process the input feature sequence that is prepared via frame-wise concatenation of the unimodal embeddings, whereas, in the prediction fusion, different unimodal temporal models (GRU+FC) are applied separately, and their output softmax label distributions are aggregated into the final predictions. The context fusion implementation has two different GRU blocks, but a common FC layer. As shown in Figure 2, COLD fusion is similar to the context fusion, but with the GRU block's output layer modified to predict the mean and variance vectors. Note that we trained the unimodal output branches simultaneously along with the fusion branch in all the multimodal models (see Figure 2).

1. Pretrained models of Toisoul et al. [71] are available at <https://github.com/face-analysis/emonet>

Data Augmentation. We applied strong data augmentation techniques to the audiovisual inputs to minimise the overfitting problem. It is important to note that under heavy overfitting, the COLD loss function (Equation (6)) may collapse, since the calibration and ordinality constraints rely on the prediction errors of the training instances. For face image data, we applied horizontal flipping with the probability set to 0.5, random scaling by a factor of 0.25, random translation by ± 30 pixels, and random rotation by 30° . In the audio case, we applied SpecAugment [77] which directly augments the 2D spectrogram itself, instead of its original 1D waveform. Here, we applied the standard SpecAugment operations: time warping, frequency masking and time masking, with their order defined arbitrarily. The parameters² of time warping (ω), frequency masking (f), and time masking (t) are chosen from different uniform distributions in the range $[0, 50]$, $[0, 27]$, and $[0, 40]$ respectively.

5.4 Optimisation Details

We used input sequences of 30 seconds duration with per-frame and per-sequence targets for the AVEC 2019 and IEMOCAP models, respectively. The visual and audio backbones and all the fusion models are trained using the Adam optimiser [78] by jointly minimising the CCC loss [63] and mean squared error for the regression task and class-weighted cross-entropy loss for the classification task. For finding the optimal values of hyper-parameters, we used the IEMOCAP validation set and the same optimal values are applied to the models trained on the AVEC 2019 corpus. The batch size, learning rate, and weight decay values chosen for training all these models are 4, $5e-3$, and $1e-4$, respectively. For tuning the learning rate, we used Cosine annealing coupled with warm restarts [79] (the number of epochs for the first restart set to 1 and the multiplication factor set to 2). The hyper-parameter values in the loss function (Eq. 6) are tuned on the logarithmic scale in the range $[1e-5, 1e+5]$ using RayTune [80]. Based on the IEMOCAP validation set performance, the following values are found to be optimal: $1e-3$ for λ_{CO_V} , λ_{CO_A} and $\lambda_{CO_{AV}}$, and $1e-4$ for λ_R . We applied the same hyperparameter values to the models trained on the AVEC 2019 corpus as well.

6 RESULTS AND DISCUSSION

We first present the results of dimensional emotion regression and classification models based on different audiovisual fusion techniques. By inducing visual noise through face masking, we investigate the robustness of the proposed COLD fusion compared to the standard fusion baselines. Then, we analyse the uncertainty calibration performance of the COLD fusion model, particularly in classification settings. To validate the improvements achieved by COLD fusion over the remaining fusion models, we conduct statistical significance tests. Furthermore, we provide a comparison between the proposed COLD fusion and a multimodal transformer baseline [81]. Finally, we present an ablation study of different components in the COLD fusion formulation, by nullifying different hyperparameters to modify the COLD training objective (Equation (8)).

2. ω – warping length, f – number of consecutive mel frequency channels masked, t – number of consecutive time steps masked

Model	Valence CCC \uparrow	Arousal CCC \uparrow	Avg. CCC \uparrow
AVEC CES Winners:Aud [82]	0.388	0.518	0.453
Aud-branch	0.369	0.465	0.417
AVEC CES Winners:Vis [82]	0.579	0.594	0.586
Vis-branch	0.511	0.514	0.512
AVEC CES Winners:AV Fusion [82]	0.614	0.645	0.629
AV Feature Fusion	0.515	0.509	0.512
AV Prediction Fusion	0.552	0.617	0.584
AV Context Fusion	0.578	0.620	0.599
AV COLD Fusion	0.611	0.661	0.636

TABLE 1: Dimensional emotion *regression* results on the **AVEC 2019 CES validation set** (CCC – Concordance Correlation Coefficient).

Model	Valence CCC \uparrow	Arousal CCC \uparrow	Avg. CCC \uparrow
Aud-branch	0.694	0.453	0.573
Vis-branch	0.496	0.355	0.425
AV Feature Fusion	0.568	0.390	0.479
AV Prediction Fusion	0.696	0.481	0.578
AV Context Fusion	0.690	0.487	0.588
AV COLD Fusion	0.723	0.504	0.613

TABLE 2: Dimensional emotion *regression* results on the **IEMOCAP test set** (CCC – Concordance Correlation Coefficient).

6.1 Dimensional Emotion Recognition Results

Regression performance of different unimodal (Aud-branch and Vis-branch) and multimodal (AV) predictions are presented in Table 1 and Table 2 for the AVEC 2019 CES (spontaneous emotion recognition) and IEMOCAP (acted emotion recognition) corpora, respectively. In both cases, COLD fusion consistently outperformed the standard fusion baselines (feature, prediction and context) as well as the unimodal results. When compared to the best performing CNN+RNN fusion baselines, on average, COLD fusion achieved $\sim 6\%$ relative improvement in dimensional emotion regression.

Compared to the winners of the AVEC 2019 challenge, Zhao et al. [82], COLD fusion performs well in terms of arousal and mean CCC scores. However, it is slightly worse in the case of valence CCC. Note that Zhao et al. [82] use a domain adaptation technique to cope with the cross-cultural variations in the audiovisual emotion expressions. However, our focus is not on coping with the cross-cultural variations, but primarily on improving the fusion performance. It is important to note that our fusion technique is, in principle, complementary to the domain adaptation used in [82]. More advanced temporal models such as Affective Processes [33], [34], [37] demonstrated superior generalisation performance than the RNNs in recent years. However, since this work mainly focuses on capturing temporal uncertainty for model-agnostic fusion based on simple CNN+RNN formulations, such

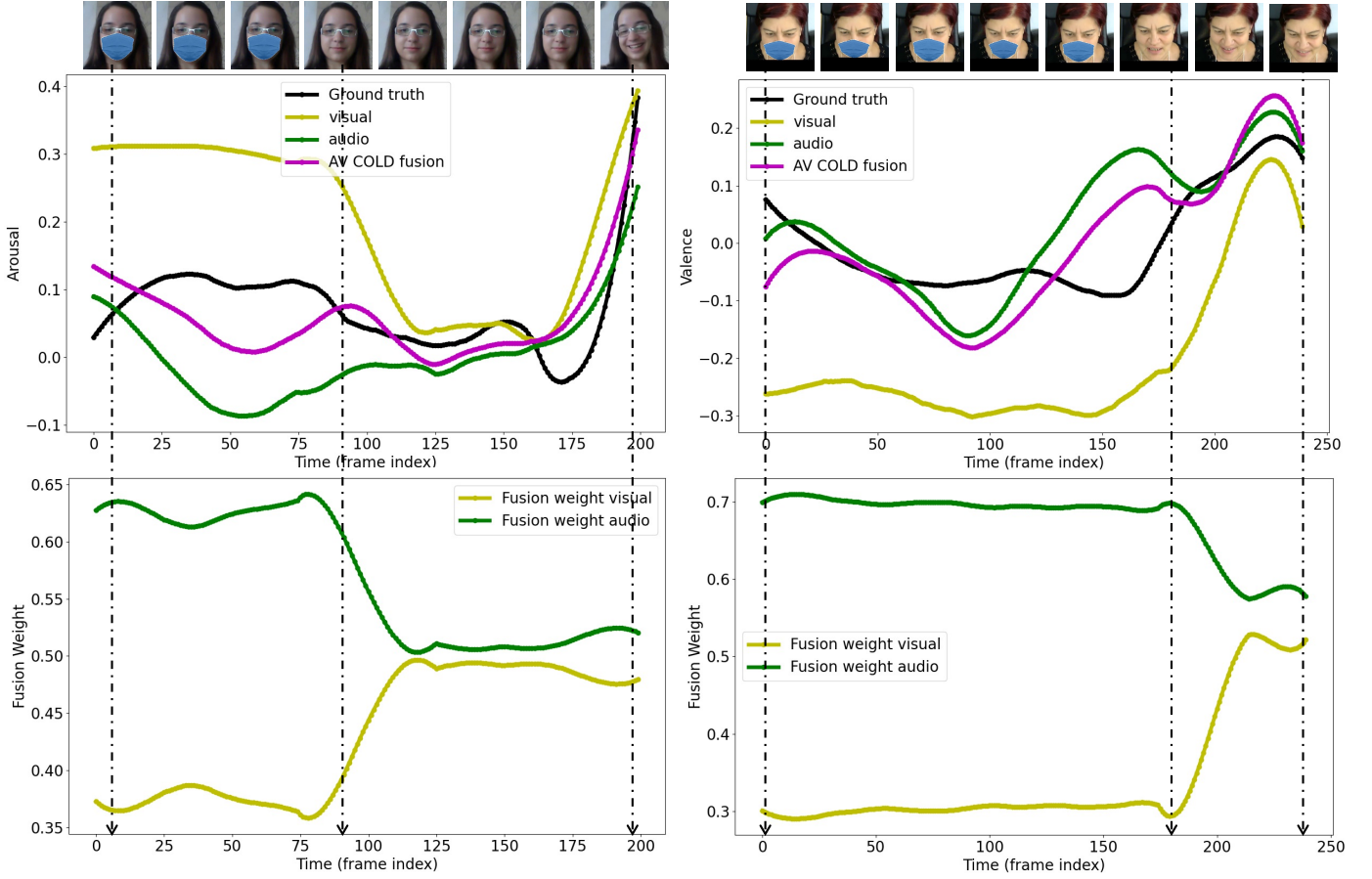


Fig. 5: Dynamic adaptation of COLD fusion weights when presented with novel noise patterns induced into the visual inputs: At test time, face masking is applied to randomly chosen consecutive frames in the AVEC 2019 CES validation examples. When the visual modality is noisy, i.e., containing faces with masks, AV COLD fusion output relies more on the audio modality (note the gaps between visual predictions and AV COLD fusion predictions, and modality-wise fusion weights). After removing the face masks, the fusion weight values adapt accordingly, hence, the fusion outputs.

Model	Valence			Arousal		
	P↑	R↑	F1↑	P↑	R↑	F1↑
Aud-branch	68.3	48.2	56.6	74.3	50.2	59.9
Vis-branch	70.9	58.1	63.9	76.8	70.3	73.4
AV Feature Fusion	67.8	60.2	63.8	73.4	68.2	70.7
AV Prediction Fusion	68.9	60.5	64.4	77.0	69.4	73.0
AV Context Fusion	75.0	60.6	67.0	77.1	71.1	73.9
AV COLD Fusion	76.8	62.4	68.9	79.5	74.0	76.5

TABLE 3: Dimensional emotion 3-way classification results (P – Precision, R – Recall, F1 – F1 score) on the AVEC 2019 CES validation set.

Model	Valence			Arousal		
	P↑	R↑	F1↑	P↑	R↑	F1↑
Aud-branch	55.5	55.3	55.4	62.4	55.1	58.5
Vis-branch	53.7	48.7	51.0	56.8	49.2	52.7
AV Feature Fusion	62.8	47.8	54.3	58.4	54.2	56.2
AV Prediction Fusion	64.5	57.3	60.7	58.9	57.0	57.9
AV Context Fusion	64.3	61.6	62.9	61.8	55.6	58.6
AV COLD Fusion	66.3	61.5	63.8	64.9	59.5	62.1

TABLE 4: Dimensional emotion 3-way classification results (P – Precision, R – Recall, F1 – F1 score) on the IEMOCAP test set.

complex temporal models based on APs are not included in this comparison, to not clutter the analysis of standard model-agnostic fusion methods presented here.

Classification performance on the AVEC 2019 CES and IEMOCAP corpora is presented in Tables 3 and 4. Similar to the regression results, COLD fusion demonstrates superior emotion classification results on both datasets. Note that here, we pose the original regression problem as a 3-way classification problem by discretising the

continuous emotion labels. For this reason, we do not have any existing benchmarks for comparison in this particular classification setting. Nevertheless, it is worth noting that the performance improvements achieved by the COLD fusion are consistent for both valence and arousal in terms of all three metrics, except for the valence recall on IEMOCAP.

Unimodal Performance Analysis. It is interesting to note that in the AVEC 2019 case, the visual modality (Vis-

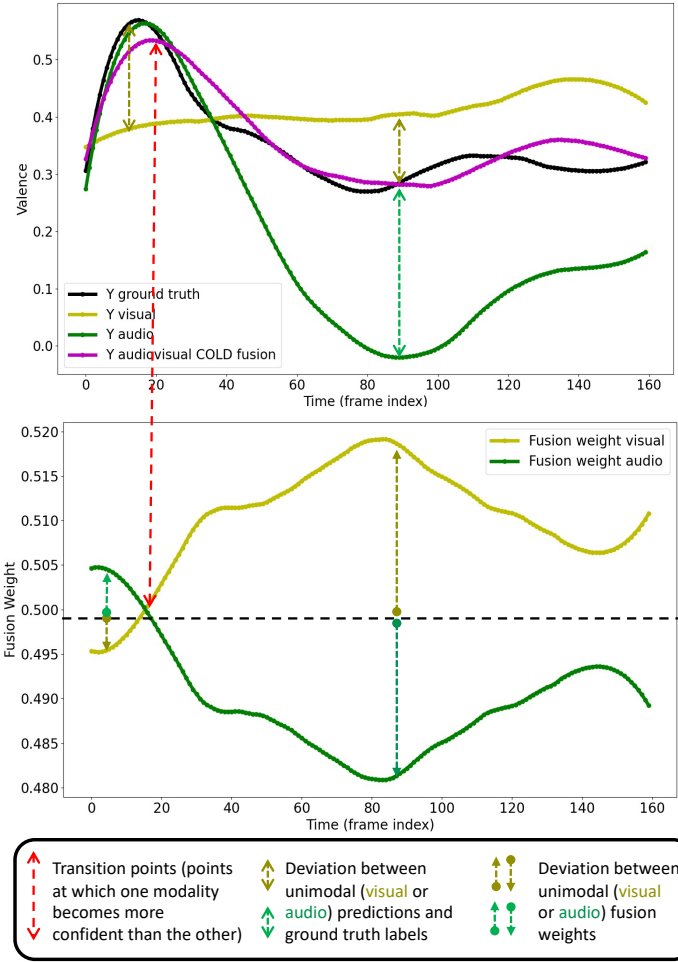


Fig. 6: Emotion predictions on an example from the AVEC 2019 CES validation set: Unimodal and multimodal valence predictions, and their uncertainty-based fusion weights estimated by the AV COLD fusion predictions. Note that fusion weights of the audio and visual modalities demonstrate (a) the calibration property – how far their corresponding unimodal predictions are from the ground truth ratings and (b) the ordinal ranking property – how well they can order the audio and visual modalities in terms of their reliability.

branch) has a considerably better recognition performance compared to the audio modality (Aud-branch), while it is vice versa in the case of the IEMOCAP dataset. This discrepancy may be due to the difference in the quality of the video data in terms of face image resolution. Despite such dataset-specific differences, our COLD fusion technique provides consistent performance improvements in the multimodal classification and regression settings for both datasets.

Analysis of Fusion Baselines. Among the fusion methods that we evaluated here, temporal context or simply context fusion is found to be the second-best performing method after the proposed COLD fusion, on both datasets. Note that here, the temporal context refers to the output of the unimodal GRU block, and unimodal predictions are generated by applying a shallow fully connected network

Model	Valence ECE ↓		Arousal ECE ↓	
	BTS	ATS	BTS	ATS
Aud-branch	13.6e-2	6.3e-2	3.2e-2	2.8e-2
Vis-branch	8.9e-2	7.1e-2	12.6e-2	3.1e-2
AV Feature Fusion	6.1e-2	5.0e-2	5.5e-2	3.3e-2
AV Prediction Fusion	8.7e-2	5.1e-2	2.5e-2	2.6e-2
AV Context Fusion	6.9e-2	4.0e-2	6.3e-2	3.0e-2
AV COLD Fusion	3.7e-2	4.3e-2	1.3e-2	0.9e-2

TABLE 5: Dimensional emotion classification *calibration* results on the AVEC 2019 CES validation set (ECE – Expected Calibration Error, BTS – Before Temperature Scaling, ATS – After Temperature Scaling).

Model	Valence ECE ↓		Arousal ECE ↓	
	BTS	ATS	BTS	ATS
Aud-branch	7.4e-2	6.0e-2	13.2e-2	8.1e-2
Vis-branch	8.0e-2	4.1e-2	7.4e-2	5.0e-2
AV Feature Fusion	7.5e-2	5.6e-2	7.0e-2	5.8e-2
AV Prediction Fusion	8.4e-2	6.4e-2	8.4e-2	4.2e-2
AV Context Fusion	9.7e-2	6.6e-2	7.9e-2	6.0e-2
AV COLD Fusion	6.1e-2	3.8e-2	1.1e-2	2.0e-2

TABLE 6: Dimensional emotion classification *calibration* results on the IEMOCAP test set (ECE – Expected Calibration Error, BTS – Before Temperature Scaling, ATS – After Temperature Scaling).

to the unimodal context vector. Thus, the context vectors can be viewed as higher-dimensional descriptors of the final unimodal predictions. Based on this assumption, in theory, the performance of context fusion is bound to be either better or at least as good as the prediction fusion, justifying the trends observed in our experimental results.

We notice that the feature fusion performance is inferior to all the remaining fusion techniques, and prediction fusion performs better than feature fusion. This result is consistent with an observation that prediction fusion achieves better results compared to feature fusion in general, as reported in the existing multimodal affect recognition literature [60]. It is worth noting that the results of feature fusion are worse than that of the best performing unimodal models on both datasets, i.e., the visual (Vis-branch) model on AVEC 2019 and the audio (Aud-branch) model on IEMOCAP. This performance degradation may be due to not explicitly correcting the temporal misalignment effects [59], which are heuristically derived in general [3]. This result indicates that integrating multimodal emotion information at feature-level or frame-level could be suboptimal most likely due to the temporal misalignment issues, given that continuous emotion information is expressed in the audiovisual modalities at different frame rates [7], [61].

Dynamic Adaptation of Fusion Weights in the Presence of Noise. In this experiment, we aim to understand how different fusion models perform when presented with novel noise patterns at test time. By inducing noise into the visual modality through face masking, here, we investigate the performance of different fusion baselines in comparison

Model	Valence CCC \uparrow	Arousal CCC \uparrow	Avg. CCC \uparrow
AV Feature Fusion	0.378	0.351	0.364
AV Prediction Fusion	0.363	0.545	0.454
AV Context Fusion	0.385	0.508	0.445
AV COLD Fusion	0.491	0.574	0.528

TABLE 7: Impact of visual noise (external occlusions) on the AV fusion models: Dimensional emotion regression results with 50% of randomly chosen face images masked during evaluation (see Fig. 5) on the AVEC 2019 CES validation Set.

with the COLD fusion. For this evaluation, we overlaid the face masks as external occlusions on the image sequences using the method proposed in MaskTheFace [83]³. We applied MaskTheFace to 50% of the randomly chosen consecutive frames of the AVEC 2019 CES validation set sequences, as shown in Figure 5. Note that all the fusion models evaluated here have not seen faces with masks during their training. As Table 7 shows, in this noise-induced evaluation set up, performance drop compared to the noise-free evaluation (Table 1) is considerably higher for all three fusion baselines (feature, prediction, and context) than for the COLD fusion. Furthermore, the relative performance difference between the COLD fusion and the best performing fusion baselines is increased from $\sim 6\%$ in noise-free settings to $\sim 17\%$ in this noise-induced case.

Figure 5 compares the COLD fusion predictions with the predictions from visual and audio branches, along with the inferred modality-wise fusion weight scores. We can clearly see that the visual fusion weights are much lower for the frames with masks compared to the frames without masks, and as a result, the final predictions rely more on the audio modality in the presence of visual noise. This result clearly demonstrates the ability of COLD fusion to dynamically adjust the importance of a specific modality according to its informativeness towards recognising the target emotions.

6.2 Uncertainty Calibration Performance Analysis

To measure the quality of uncertainty estimates, we computed Expected Calibration Error (ECE) (see Section 5.2) values for the unimodal and multimodal emotion classification models. Note that this calibration error metric applies only to the classification settings. By computing the ECE values before and after applying temperature scaling to the softmax distributions over the predictions of each model separately, we analyse the impact of explicit uncertainty calibration (temperature scaling). We searched for an optimal temperature value in the range of $1e-2$ to 1000 by doing a random search for 100 iterations. Similar to the technique followed in [12], we selected a temperature value that achieves the lowest ECE value on the validation set.

It is important to consider that the COLD fusion models are trained to be implicitly calibrated (see Equation (6)) in terms of their context variance values. Thus, even before applying explicit calibration, i.e., temperature scaling, we expect the predictive uncertainty values or class wise

Model	Valence CCC \uparrow	Arousal CCC \uparrow
With All three constraints ($\lambda_{CV} = \lambda_{CA} = \lambda_{CAV} = 1e-3$, $\lambda_R = 1e-4$)	0.605	0.661
Without Intramodal constraints ($\lambda_{CV} = \lambda_{CA=0}$)	0.573	0.615
Without Crossmodal constraint (λ_{CAV})	0.580	0.609
Without Regularisation constraint ($\lambda_R = 0$)	0.541	0.595
Without Any constraints ($\lambda_{CV} = \lambda_{CA} = \lambda_{CAV} = 0$, $\lambda_R = 0$)	0.517	0.578

TABLE 8: Ablation experiments on the proposed loss function (Eq. 6): Analysing the impact of different loss components in the COLD Fusion on the AVEC 2019 CES validation set (CCC-Concordance Correlation Coefficient).

Model	Valence CCC \uparrow	Arousal CCC \uparrow	Avg. CCC \uparrow
Multimodal AV Transformer [81] [†]	0.602	0.619	0.610
Proposed AV COLD Fusion	0.611	0.661	0.636

TABLE 9: Comparison with a pair-wise crossmodal self-attention based multimodal transformer [81] ([†] indicates in-house implementation for AV fusion): Regression results on the AVEC 2019 CES validation set.

confidence scores of the COLD fusion models to have lower ECE values compared to the other fusion baselines.

Quantitative Results. Table 5 reports the ECE values for valence and arousal attributes on the AVEC 2019 corpus. For both the attributes, before the application of temperature scaling, COLD fusion has the lowest calibration error when compared to the other models. After applying temperature scaling, it is obvious that the ECE values for all the models go down, and the COLD fusion still achieves the lowest error. Only in the case of valence, AV context fusion has a marginally lower ECE value compared to the COLD fusion. This minor discrepancy could be due to the random search of optimal temperature values and note that here, different models have different optimal temperature values that are tuned for valence and arousal, separately. Nevertheless, in all the remaining cases (both before and after temperature scaling), COLD fusion consistently demonstrates lower uncertainty calibration errors in relation to the other fusion models. Results on the IEMOCAP corpus, as shown in Table 6, follow similar trends, validating the effectiveness of the COLD fusion approach in producing well-calibrated uncertainty estimates.

Reliability diagrams visually illustrate the uncertainty calibration performance of a model’s predictions. As Figure 7 shows, when a model is perfectly calibrated, its confidence score vs the accuracy score histogram looks like a perfect right-angled triangle. The more the deviations are from the diagonal lines in them, the higher their ECE values are. Note that ECE is a scalar summary statistic of a reliability diagram, which computes the weighted average of such deviations over all the intervals in the reliability diagram. Though the ECE values reported for both the

3. <https://github.com/aeqelanwar/MaskTheFace>

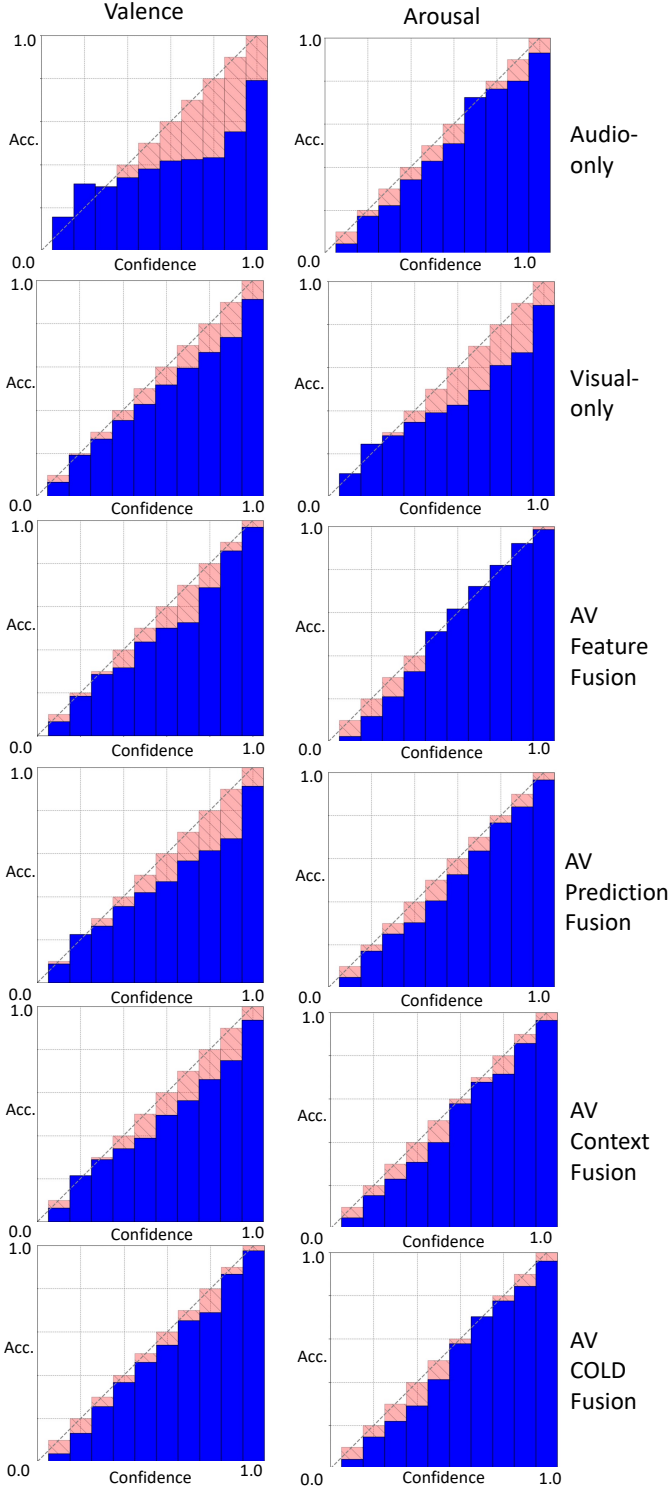


Fig. 7: Reliability plots of unimodal and multimodal classification models evaluated on the AVEC 2019 validation set. A perfectly calibrated model appears as a perfect right angled triangle, as marked by the diagonal lines and the red bars.

Model Pair	Valence p-Value ↓	Arousal p-Value ↓
(Aud-branch, AV COLD Fusion)	6.4e-34	9.7e-23
(Vis-branch, AV COLD Fusion)	1.9e-15	3.3e-16
(AV Feature Fusion, AV COLD Fusion)	3.7e-14	1.1e-18
(AV Prediction Fusion, AV COLD Fusion)	5.5e-9	7.3e-3
(AV Context Fusion, AV COLD Fusion)	1.2e-4	2.0e-3
(AV COLD Fusion, AV COLD Fusion)	1.0e-0	1.0e-0

TABLE 10: Statistical significance testing ($p < 0.01$): Regression t -test results on the AVEC 2019 CES validation set.

AVEC 2019 corpus (Table 5) and IEMOCAP (Table 6) already validate the improved calibration results with COLD fusion. Here, as an example, in Figure 7 we compare the reliability plots of different models evaluated on the AVEC validation set. In Figure 7, we can see that compared to the unimodal cases and other fusion baselines, the COLD fusion reliability plot looks much closer to a perfect right-angled triangle. Among all the reliability plots illustrated, we observe that the audio branch for valence has the highest calibration error. This observation is in line with the poor performance achieved by the audio modality in terms of the valence prediction error (see Table 1 and Table 3) on the AVEC 2019 corpus.

Analysis of Audiovisual Fusion Weights. In Figure 6, we qualitatively illustrate modality-wise fusion weights estimated by the COLD fusion model on a validation sequence taken from the AVEC 2019 corpus. Note that these fusion weights are functions of the unimodal temporal context distributions (see Equation (2)). In this illustration, we analyse the temporal patterns of fusion weights along with their corresponding unimodal and multimodal emotion predictions and their ground truth labels. This analysis clearly shows the well-calibrated nature of modality-wise fusion weights: when the predictions of one modality move closer to the ground truth compared to those of the other modality, the audiovisual weight values in the COLD fusion are found to be varying accordingly. From the transition points marked in Figure 6, we can see that the fusion weights are gradually inverted, as the predictions of one modality move closer to the ground truth while the other modality predictions move further. This result validates our main hypothesis of making unimodal latent distributions calibrated and ordinal for improved fusion performance.

Statistical Significance Analysis. As shown in Table 10, we conducted paired t -test on the validation set of the AVEC 2019 corpus, to verify the statistical significance of COLD fusion’s performance improvements over the unimodal and remaining multimodal baselines. In line with the trends in regression, performance reported in Table 1, p-values of the student t -test indicate that the improvements achieved by the COLD fusion models are statistically quite significant compared to the baseline models.

Comparison with a Multimodal Transformer [81]. In

addition to the standard fusion baselines, we implemented a multimodal transformer model based on pair-wise crossmodal self-attention fusion proposed in Tsai et al. [81]. It is worth noting that the crossmodal self-attention fusion aims to cope with the problem of temporal misalignment between different modalities during fusion, similar to the temporal context fusion model we evaluated in this work. We implemented an audio-visual version of this multimodal transformer method by tailoring its original network architecture designed for the text, audio, and visual modalities⁴. We used a 3-layer self-attention network with 16 heads followed by an FC output layer to implement this multimodal transformer baseline. As shown in Table 9, regression results on the AVEC 2019 CES corpus show that the COLD fusion clearly outperformed the transformer baseline, particularly in arousal prediction, by a large margin.

Ablation Studies. Table 8 presents the ablation results that quantify the contributions of calibration, ordinality, and variance regularisation constraints to the performance gains achieved by COLD fusion. By individually nullifying the four optimisation hyperparameters of the COLD training objective (see Equation (8)), we measure the emotion regression performance on the AVEC 2019 validation set. Compared to the fully constrained COLD fusion model, different partially constrained and fully unconstrained models listed in Table 8, achieve considerably lower CCC scores. Most importantly, we observe that discarding the variance regularisation constraint results in more performance degradation than the remaining constraints. This observation indicates the importance of preventing the variance collapse problem by using the variance regularisation term, in line with the results reported in prior works [33], [65].

7 CONCLUSION

We proposed an uncertainty-aware multimodal fusion approach to dimensional emotion recognition from audiovisual data. To capture modality-wise uncertainty w.r.t. predicting valence and arousal dimensions, we probabilistically modelled the temporal context of faces and voices by learning unimodal latent distributions. For effective uncertainty-weighted audiovisual fusion, we suggested to condition the unimodal latent distributions such that their variance norms are learnt to be *well-calibrated* and *well-ranked* (ordinal). To jointly impose these two constraints on the latent distributions, we introduced a novel softmax distributional matching loss function that encourages the uncertainty scores to be well-calibrated and well-ranked. Our novel loss function for multimodal learning is applicable to both classification and regression settings.

On spontaneous and acted emotion recognition tasks, our proposed uncertainty-aware fusion model achieved significantly better recognition performance than the uncertainty-unaware model-agnostic fusion baselines, including a multimodal transformer [81]. Validating our main hypothesis, extensive ablation studies showed that it is important to apply both calibration and ordinality constraints for improving the emotion recognition results of

uncertainty-aware fusion models. Furthermore, our method demonstrated noticeable improvements in terms of predictive uncertainty calibration errors of the emotion recognition models. It is important to note that our proposed calibration and ordinal ranking constraints can be easily applied to general model-fusion methods as well by quantifying the model-wise predictive uncertainty values of emotion labels.

In summary, this work showed the importance of uncertainty modelling for the dynamic integration of emotional expression cues from multimodal signals. We believe that uncertainty-aware information fusion is fundamental to reliably recognise apparent emotional states in naturalistic conditions. We hope that the results we demonstrated in this work may help in generating more interest in embracing uncertainty in multimodal affective computing.

ACKNOWLEDGMENTS

The work of Mani Kumar Tellamekala was supported by the Engineering and Physical Science Research Council project (2159382) and Unilever U.K. Ltd, and the work of Michel Valstar was supported by the Nottingham Biomedical Research Centre (BRC).

REFERENCES

- [1] B. Schuller, M. Valster, F. Eyben, R. Cowie, and M. Pantic, "Avec 2012: the continuous audio/visual emotion challenge," in *Proceedings of the 14th ACM international conference on Multimodal interaction*, 2012, pp. 449–456.
- [2] M. Valstar, B. Schuller, K. Smith, F. Eyben, B. Jiang, S. Bilakhia, S. Schnieder, R. Cowie, and M. Pantic, "Avec 2013: the continuous audio/visual emotion and depression recognition challenge," in *Proceedings of the 3rd ACM international workshop on Audio/visual emotion challenge*, 2013, pp. 3–10.
- [3] F. Ringeval, B. Schuller, M. Valstar, N. Cummins, R. Cowie, L. Tavabi, M. Schmitt, S. Alisamir, S. Amiriparian, E.-M. Messner et al., "Avec 2019 workshop and challenge: state-of-mind, detecting depression with ai, and cross-cultural affect recognition," in *Proceedings of the 9th International on Audio/Visual Emotion Challenge and Workshop*, 2019, pp. 3–12.
- [4] S. K. D'mello and J. Kory, "A review and meta-analysis of multimodal affect detection systems," *ACM Computing Surveys (CSUR)*, vol. 47, no. 3, pp. 1–36, 2015.
- [5] M. A. Nicolaou, H. Gunes, and M. Pantic, "Continuous prediction of spontaneous affect from multiple cues and modalities in valence-arousal space," *IEEE Transactions on Affective Computing*, vol. 2, no. 2, pp. 92–105, 2011.
- [6] Z. Zeng, M. Pantic, G. I. Roisman, and T. S. Huang, "A survey of affect recognition methods: Audio, visual, and spontaneous expressions," *IEEE transactions on pattern analysis and machine intelligence*, vol. 31, no. 1, pp. 39–58, 2008.
- [7] P. V. Rouast, M. Adam, and R. Chiong, "Deep learning for human affect recognition: Insights and new developments," *IEEE Transactions on Affective Computing*, 2019.
- [8] F. Noroozi, M. Marjanovic, A. Njegus, S. Escalera, and G. Anbarjafari, "Audio-visual emotion recognition in video clips," *IEEE Transactions on Affective Computing*, vol. 10, no. 1, pp. 60–75, 2017.
- [9] L. Schoneveld, A. Othmani, and H. Abdelkawy, "Leveraging recent advances in deep learning for audio-visual emotion recognition," *Pattern Recognition Letters*, vol. 146, pp. 1–7, 2021.
- [10] M. Gerczuk, S. Amiriparian, S. Ottl, and B. W. Schuller, "Emonet: A transfer learning framework for multi-corpus speech emotion recognition," *IEEE Transactions on Affective Computing*, 2021.
- [11] C. Guo, G. Pleiss, Y. Sun, and K. Q. Weinberger, "On calibration of modern neural networks," in *International Conference on Machine Learning*. PMLR, 2017, pp. 1321–1330.
- [12] J. Mukhoti, V. Kulharia, A. Sanyal, S. Golodetz, P. H. Torr, and P. K. Dokania, "Calibrating deep neural networks using focal loss," *arXiv preprint arXiv:2002.09437*, 2020.

4. <https://github.com/yaohungt/Multimodal-Transformer>

- [13] A. Nguyen, J. Yosinski, and J. Clune, "Deep neural networks are easily fooled: High confidence predictions for unrecognizable images," in *Proceedings of the IEEE conference on computer vision and pattern recognition*, 2015, pp. 427–436.
- [14] C. Szegedy, W. Zaremba, I. Sutskever, J. Bruna, D. Erhan, I. Goodfellow, and R. Fergus, "Intriguing properties of neural networks," *arXiv preprint arXiv:1312.6199*, 2013.
- [15] A. Kumar, S. Sarawagi, and U. Jain, "Trainable calibration measures for neural networks from kernel mean embeddings," in *International Conference on Machine Learning*. PMLR, 2018, pp. 2805–2814.
- [16] J. Moon, J. Kim, Y. Shin, and S. Hwang, "Confidence-aware learning for deep neural networks," in *international conference on machine learning*. PMLR, 2020, pp. 7034–7044.
- [17] X. Yang, P. Ramesh, R. Chitta, S. Madhvanath, E. A. Bernal, and J. Luo, "Deep multimodal representation learning from temporal data," in *Proceedings of the IEEE conference on computer vision and pattern recognition*, 2017, pp. 5447–5455.
- [18] C. Busso, M. Bulut, C.-C. Lee, A. Kazemzadeh, E. Mower, S. Kim, J. N. Chang, S. Lee, and S. S. Narayanan, "Iemocap: Interactive emotional dyadic motion capture database," *Language resources and evaluation*, vol. 42, no. 4, pp. 335–359, 2008.
- [19] H. Gunes, B. Schuller, M. Pantic, and R. Cowie, "Emotion representation, analysis and synthesis in continuous space: A survey," in *2011 IEEE International Conference on Automatic Face & Gesture Recognition (FG)*. IEEE, 2011, pp. 827–834.
- [20] L. Stappen, A. Baird, G. Rizos, P. Tzirakis, X. Du, F. Hafner, L. Schumann, A. Mallol-Ragolta, B. W. Schuller, I. Lefter *et al.*, "Muse 2020 challenge and workshop: Multimodal sentiment analysis, emotion-target engagement and trustworthiness detection in real-life media: Emotional car reviews in-the-wild," in *Proceedings of the 1st International on Multimodal Sentiment Analysis in Real-life Media Challenge and Workshop*, 2020, pp. 35–44.
- [21] L. Stappen, A. Baird, L. Christ, L. Schumann, B. Sertolli, E.-M. Messner, E. Cambria, G. Zhao, and B. W. Schuller, "The muse 2021 multimodal sentiment analysis challenge: sentiment, emotion, physiological-emotion, and stress," in *Proceedings of the 2nd on Multimodal Sentiment Analysis Challenge*, 2021, pp. 5–14.
- [22] L. Christ, S. Amiriparian, A. Baird, P. Tzirakis, A. Kathan, N. Müller, L. Stappen, E.-M. Meßner, A. König, A. Cowen *et al.*, "The muse 2022 multimodal sentiment analysis challenge: Humor, emotional reactions, and stress," 2022.
- [23] D. Kollias, A. Schulc, E. Hajiyeve, and S. Zafeiriou, "Analysing affective behavior in the first abaw 2020 competition," *arXiv preprint:2001.11409*, 2020.
- [24] D. Kollias and S. Zafeiriou, "Analysing affective behavior in the second abaw2 competition," in *Proceedings of the IEEE/CVF International Conference on Computer Vision*, 2021, pp. 3652–3660.
- [25] S. Poria, E. Cambria, R. Bajpai, and A. Hussain, "A review of affective computing: From unimodal analysis to multimodal fusion," *Information Fusion*, vol. 37, pp. 98–125, 2017.
- [26] J. She, Y. Hu, H. Shi, J. Wang, Q. Shen, and T. Mei, "Dive into ambiguity: Latent distribution mining and pairwise uncertainty estimation for facial expression recognition," in *Proceedings of the IEEE/CVF Conference on Computer Vision and Pattern Recognition*, 2021, pp. 6248–6257.
- [27] Y. Zhang, C. Wang, and W. Deng, "Relative uncertainty learning for facial expression recognition," *Advances in Neural Information Processing Systems*, vol. 34, 2021.
- [28] K. Wang, X. Peng, J. Yang, S. Lu, and Y. Qiao, "Suppressing uncertainties for large-scale facial expression recognition," in *Proceedings of the IEEE/CVF Conference on Computer Vision and Pattern Recognition*, 2020, pp. 6897–6906.
- [29] N. M. Foteinopoulou, C. Tzelepis, and I. Patras, "Estimating continuous affect with label uncertainty," in *2021 9th International Conference on Affective Computing and Intelligent Interaction (ACII)*. IEEE, 2021, pp. 1–8.
- [30] Z. Zeng, J. Tu, M. Liu, and T. S. Huang, "Multi-stream confidence analysis for audio-visual affect recognition," in *International Conference on Affective Computing and Intelligent Interaction*. Springer, 2005, pp. 964–971.
- [31] Z. Xie and L. Guan, "Multimodal information fusion of audiovisual emotion recognition using novel information theoretic tools," in *2013 IEEE International Conference on Multimedia and Expo (ICME)*. IEEE, 2013, pp. 1–6.
- [32] T. Dang, B. Stasak, Z. Huang, S. Jayawardena, M. Atcheson, M. Hayat, P. Le, V. Sethu, R. Goecke, and J. Epps, "Investigating word affect features and fusion of probabilistic predictions incorporating uncertainty in avec 2017," in *Proceedings of the 7th Annual Workshop on Audio/Visual Emotion Challenge*, 2017, pp. 27–35.
- [33] E. Sanchez, M. K. Tellamekala, M. Valstar, and G. Tzimiropoulos, "Affective processes: stochastic modelling of temporal context for emotion and facial expression recognition," in *CVPR*, 2021.
- [34] T. Mani Kumar, E. Sanchez, G. Tzimiropoulos, T. Giesbrecht, and M. Valstar, "Stochastic process regression for cross-cultural speech emotion recognition," *Proc. Interspeech 2021*, pp. 3390–3394, 2021.
- [35] M. Garnelo, D. Rosenbaum, C. Maddison, T. Ramalho, D. Saxton, M. Shanahan, Y. W. Teh, D. Rezende, and S. A. Eslami, "Conditional neural processes," in *ICML*, 2018, pp. 1704–1713.
- [36] M. Garnelo, J. Schwarz, D. Rosenbaum, F. Viola, D. J. Rezende, S. M. A. Eslami, and Y. W. Teh, "Neural processes," in *ICML Workshop on Theoretical Foundations and Applications of Deep Generative Models*, 2018.
- [37] M. K. Tellamekala, T. Giesbrecht, and M. Valstar, "Modelling stochastic context of audio-visual expressive behaviour with affective processes," *IEEE Transactions on Affective Computing*, no. 01, pp. 1–1, 2022.
- [38] A. Schörgendorfer and W. Elmenreich, *Extended confidence-weighted averaging in sensor fusion*. na, 2006.
- [39] P. W. Große, H. Holzapfel, and A. Waibel, "Confidence based multimodal fusion for person identification," in *Proceedings of the 16th ACM international conference on Multimedia*, 2008, pp. 885–888.
- [40] G. Papandreou, A. Katsamanis, V. Pitsikalis, and P. Maragos, "Adaptive multimodal fusion by uncertainty compensation with application to audiovisual speech recognition," *IEEE Transactions on Audio, Speech, and Language Processing*, vol. 17, no. 3, pp. 423–435, 2009.
- [41] M. Subedar, R. Krishnan, P. L. Meyer, O. Tickoo, and J. Huang, "Uncertainty-aware audiovisual activity recognition using deep bayesian variational inference," in *Proceedings of the IEEE/CVF International Conference on Computer Vision*, 2019, pp. 6301–6310.
- [42] J. Tian, W. Cheung, N. Glaser, Y.-C. Liu, and Z. Kira, "Uno: Uncertainty-aware noisy-or multimodal fusion for unanticipated input degradation," in *2020 IEEE International Conference on Robotics and Automation (ICRA)*. IEEE, 2020, pp. 5716–5723.
- [43] D.-B. Wang, L. Feng, and M.-L. Zhang, "Rethinking calibration of deep neural networks: Do not be afraid of overconfidence," *Advances in Neural Information Processing Systems*, vol. 34, 2021.
- [44] M. Minderer, J. Djolonga, R. Romijnders, F. Hubis, X. Zhai, N. Houlsby, D. Tran, and M. Lucic, "Revisiting the calibration of modern neural networks," *Advances in Neural Information Processing Systems*, vol. 34, 2021.
- [45] B. Zadrozny and C. Elkan, "Obtaining calibrated probability estimates from decision trees and naive bayesian classifiers," in *ICML*, vol. 1. Citeseer, 2001, pp. 609–616.
- [46] —, "Transforming classifier scores into accurate multiclass probability estimates," in *Proceedings of the eighth ACM SIGKDD international conference on Knowledge discovery and data mining*, 2002, pp. 694–699.
- [47] J. Platt *et al.*, "Probabilistic outputs for support vector machines and comparisons to regularized likelihood methods," *Advances in large margin classifiers*, vol. 10, no. 3, pp. 61–74, 1999.
- [48] G. Hinton, O. Vinyals, and J. Dean, "Distilling the knowledge in a neural network," *arXiv preprint arXiv:1503.02531*, 2015.
- [49] R. Krishnan and O. Tickoo, "Improving model calibration with accuracy versus uncertainty optimization," *arXiv preprint arXiv:2012.07923*, 2020.
- [50] V. Kuleshov, N. Fenner, and S. Ermon, "Accurate uncertainties for deep learning using calibrated regression," in *International Conference on Machine Learning*. PMLR, 2018, pp. 2796–2804.
- [51] H. Song, T. Diethe, M. Kull, and P. Flach, "Distribution calibration for regression," in *International Conference on Machine Learning*, 2019, pp. 5897–5906.
- [52] S. Utpala and P. Rai, "Quantile regularization: Towards implicit calibration of regression models," *arXiv preprint arXiv:2002.12860*, 2020.
- [53] W. Li, X. Huang, J. Lu, J. Feng, and J. Zhou, "Learning probabilistic ordinal embeddings for uncertainty-aware regression," in *Proceedings of the IEEE/CVF Conference on Computer Vision and Pattern Recognition*, 2021, pp. 13 896–13 905.
- [54] C. Corbière, N. Thome, A. Bar-Hen, M. Cord, and P. Pérez, "Addressing failure prediction by learning model confidence," *arXiv preprint arXiv:1910.04851*, 2019.

- [55] R. Roady, T. L. Hayes, R. Kemker, A. Gonzales, and C. Kanan, "Are out-of-distribution detection methods effective on large-scale datasets?" *arXiv preprint arXiv:1910.14034*, 2019.
- [56] Y. Geifman and R. El-Yaniv, "Selective classification for deep neural networks," *arXiv preprint arXiv:1705.08500*, 2017.
- [57] T. Baltrušaitis, C. Ahuja, and L.-P. Morency, "Multimodal machine learning: A survey and taxonomy," *IEEE transactions on pattern analysis and machine intelligence*, vol. 41, no. 2, pp. 423–443, 2018.
- [58] S. Zhang, S. Zhang, T. Huang, W. Gao, and Q. Tian, "Learning affective features with a hybrid deep model for audio-visual emotion recognition," *IEEE Transactions on Circuits and Systems for Video Technology*, vol. 28, no. 10, pp. 3030–3043, 2017.
- [59] F. Lingenfelder, J. Wagner, J. Deng, R. Brueckner, B. Schuller, and E. André, "Asynchronous and event-based fusion systems for affect recognition on naturalistic data in comparison to conventional approaches," *IEEE Transactions on Affective Computing*, vol. 9, no. 4, pp. 410–423, 2016.
- [60] F. Ringeval, F. Eyben, E. Kroupi, A. Yuce, J.-P. Thiran, T. Ebrahimi, D. Lalanne, and B. Schuller, "Prediction of asynchronous dimensional emotion ratings from audiovisual and physiological data," *Pattern Recognition Letters*, vol. 66, pp. 22–30, 2015.
- [61] P. Tzirakis, G. Trigeorgis, M. A. Nicolaou, B. W. Schuller, and S. Zafeiriou, "End-to-end multimodal emotion recognition using deep neural networks," *IEEE Journal of Selected Topics in Signal Processing*, vol. 11, no. 8, pp. 1301–1309, 2017.
- [62] G. Evangelopoulos, A. Zlatintsi, A. Potamianos, P. Maragos, K. Rantzikos, G. Skoumas, and Y. Avrithis, "Multimodal saliency and fusion for movie summarization based on aural, visual, and textual attention," *IEEE Transactions on Multimedia*, vol. 15, no. 7, pp. 1553–1568, 2013.
- [63] J. Kossaifi, A. Toisoul, A. Bulat, Y. Panagakis, T. M. Hospedales, and M. Pantic, "Factorized higher-order cnns with an application to spatio-temporal emotion estimation," in *CVPR*, June 2020.
- [64] S. Bruch, X. Wang, M. Bendersky, and M. Najork, "An analysis of the softmax cross entropy loss for learning-to-rank with binary relevance," in *Proceedings of the 2019 ACM SIGIR International Conference on Theory of Information Retrieval*, 2019, pp. 75–78.
- [65] J. Chang, Z. Lan, C. Cheng, and Y. Wei, "Data uncertainty learning in face recognition," in *CVPR*, 2020, pp. 5710–5719.
- [66] J. Kossaifi, R. Walecki, Y. Panagakis, J. Shen, M. Schmitt, F. Ringeval, J. Han, V. Pandit, A. Toisoul, B. W. Schuller *et al.*, "Sewa db: A rich database for audio-visual emotion and sentiment research in the wild," *IEEE Trans. Pattern Anal. Mach. Intell.*, 2019.
- [67] Z. Zhao, Y. Zheng, Z. Zhang, H. Wang, Y. Zhao, and C. Li, "Exploring spatio-temporal representations by integrating attention-based bidirectional-lstm-rnns and fcns for speech emotion recognition," 2018.
- [68] S. Tripathi and H. Beigi, "Multi-modal emotion recognition on iemocap with neural networks," *arXiv preprint arXiv:1804.05788*, 2018.
- [69] I. Lawrence and K. Lin, "A concordance correlation coefficient to evaluate reproducibility," *Biometrics*, pp. 255–268, 1989.
- [70] J. Yang, A. Bulat, and G. Tzimiropoulos, "Fan-face: a simple orthogonal improvement to deep face recognition," in *Proceedings of the AAAI Conference on Artificial Intelligence*, vol. 34, no. 07, 2020, pp. 12 621–12 628.
- [71] A. Toisoul, J. Kossaifi, A. Bulat, G. Tzimiropoulos, and M. Pantic, "Estimation of continuous valence and arousal levels from faces in naturalistic conditions," *Nature Machine Intelligence*, vol. 3, no. 1, pp. 42–50, 2021.
- [72] I. Ntinou, E. Sanchez, A. Bulat, M. Valstar, and Y. Tzimiropoulos, "A transfer learning approach to heatmap regression for action unit intensity estimation," *IEEE Transactions on Affective Computing*, 2021.
- [73] A. Mollahosseini, B. Hasani, and M. H. Mahoor, "Affectnet: A database for facial expression, valence, and arousal computing in the wild," *IEEE Transactions on Affective Computing*, vol. 10, no. 1, pp. 18–31, 2017.
- [74] H. Chen, Y. Deng, S. Cheng, Y. Wang, D. Jiang, and H. Sahli, "Efficient spatial temporal convolutional features for audiovisual continuous affect recognition," in *AVEC*, 2019, pp. 19–26.
- [75] S. Hershey, S. Chaudhuri, D. P. Ellis, J. F. Gemmeke, A. Jansen, R. C. Moore, M. Plakal, D. Platt, R. A. Saurous, B. Seybold *et al.*, "Cnn architectures for large-scale audio classification," in *ICASSP*. IEEE, 2017, pp. 131–135.
- [76] S. Chen, Q. Jin, J. Zhao, and S. Wang, "Multimodal multi-task learning for dimensional and continuous emotion recognition," in *AVEC*, 2017, pp. 19–26.
- [77] D. S. Park, W. Chan, Y. Zhang, C.-C. Chiu, B. Zoph, E. D. Cubuk, and Q. V. Le, "SpecAugment: A simple data augmentation method for automatic speech recognition," *arXiv preprint arXiv:1904.08779*, 2019.
- [78] D. P. Kingma and J. Ba, "Adam: A method for stochastic optimization," *arXiv preprint:1412.6980*, 2014.
- [79] I. Loshchilov and F. Hutter, "Sgdr: Stochastic gradient descent with warm restarts," *arXiv preprint:1608.03983*, 2016.
- [80] R. Liaw, E. Liang, R. Nishihara, P. Moritz, J. E. Gonzalez, and I. Stoica, "Tune: A research platform for distributed model selection and training," *arXiv preprint arXiv:1807.05118*, 2018.
- [81] Y.-H. H. Tsai, S. Bai, P. P. Liang, J. Z. Kolter, L.-P. Morency, and R. Salakhutdinov, "Multimodal transformer for unaligned multimodal language sequences," in *Proceedings of the conference. Association for Computational Linguistics. Meeting*, vol. 2019. NIH Public Access, 2019, p. 6558.
- [82] J. Zhao, R. Li, J. Liang, S. Chen, and Q. Jin, "Adversarial domain adaption for multi-cultural dimensional emotion recognition in dyadic interactions," in *Proceedings of the 9th International on Audio/Visual Emotion Challenge and Workshop*, 2019, pp. 37–45.
- [83] A. Anwar and A. Raychowdhury, "Masked face recognition for secure authentication," *arXiv preprint arXiv:2008.11104*, 2020.